Korea-Australia Rheology Journal, 27(2), 95-103 (May 2015) www.springer.com/13367
DOI: 10.1007/s13367-015-0010-3

Nonlinear behavior of PP/PS blends with and without clay under large amplitude oscillatory shear (LAOS) flow

Reza Salehiyan, Hyeong Yong Song and Kyu Hyun*
School of Chemical and Biomolecular Engineering, Pusan National University, Busan 609-735, Republic of Korea
(Received December 14, 2014; final revision received March 6, 2015; accepted March 16, 2015)

Dynamic oscillatory measurement, *i.e.*, small amplitude oscillatory shear (SAOS) and large amplitude oscillatory shear (LAOS) test was used to investigate linear and non-linear viscoelastic properties of Polypropylene (PP)/Polystyrene (PS) blends with and without 5 wt.% clay (C20A). Fourier transform (FT-Rheology), Lissajous curves and stress decomposition methods were used to analyze non-linear responses under LAOS flow. Composition effects of blends were investigated prior to compatibilization effects. Elevated concentrations of dispersed phase (PS) increased the moduli G'(ω) from SAOS test and G*(γ) from LAOS test of the blends as well as strain thinning behavior. Interestingly, addition of 5 wt.% clay (C20A) boosted moduli of the blends as well as led to similar strain thinning behaviors among the PP/PS/C20A blends, except for the (90/10) PP/PS blend. The latter did not show improved rheological properties despite morphological improvements, as shown by SEM. Results from SEM and improved rheological properties of PP/PS/C20A blends revealed the compatibilization effects of clay (C20A) particles regardless of size reduction mechanisms. Third relative intensities ($I_{3/1}$) from FT-rheology were found to be sensitive to clay (C20A) additions for the (70/30) and (30/70) PP/PS blends. Similarly, Lissajous curves could detect changes upon clay (C20A) addition, specifically at lower strain amplitudes whereupon addition of 5 wt.% clay resulted in the closed loops of Lissajous curves showing a more ellipsoidal shape due to increased elasticity in the blends. However, detection of these changes at larger strain amplitudes was more challenging. Therefore, stress decomposition (SD) method was applied for more precise characterization as it decomposes the total stress (σ) into elastic stress (σ') and viscous stress (σ''). Using SD method, elastic stress was more distorted, especially, strain hardening, while the total stress response remained almost unchanged at larger strain amplitudes.

Keywords: linear and non-linear viscoelastic properties, PP/PS/C20A blends, FT-rheology, composition ratio, compatibilization

1. Introduction

Multiphasic structures can be obtained as a result of mixing immiscible polymeric materials due to their unfavorable interactions. Diversity of final properties is a common result of mixing immiscible polymers whereas gaining such characteristics by using only homopolymers is a great challenge or almost impossible. Therefore, it is quite beneficial to control the morphologies of blends in order to obtain the desired material with specific properties with respect to its end-use applications. In other words, morphological evolutions could strongly affect the final performance of immiscible blends (Van Puyvelde *et al*., 2001; Souza and Demarquette, 2002).

Among different methods to characterize polymer blends, rheological properties are a promising tool to monitor morphological evolutions and microstructural changes. (Gleinser *et al*., 1994; Asthana and Jayaraman, 1999; Ziegler and Wolf, 1999; Van Puyvelde *et al*., 2001; Macaubas *et al*., 2005; Elias *et al*., 2007; 2008; Hyun and Wilhelm, 2009; Hyun *et al*., 2011).

Ziegler and Wolf (1999) previously reported the correlation between rheological properties and composition ratios of Poly(dimethylsiloxane)/Poly(dimethylsiloxane-*ran*-methylphenyl-siloxane) (PDMS/COP) blends. They observed weaker shear thinning behavior within the phase inversion composition, where the blend showed co-continuous morphology, due to less deformability.

Souza and Demarquette (2002) reported that there is a composition range for polypropylene/high density polyethylene (PP/HDPE) blends where interfacial tensions can be calculated from rheological properties. They found that there is a strong relationship between longest relaxation times obtained from experiments and those of predicted by Palierne's model within particular composition ranges. Similarly, Gui *et al*. (2012) calculated interfacial tensions of polylactic acid/poly butyelene succinate adipate (PLA/PBSA) blends using Palierne's model and the weighted relaxation spectrum and reporting consistency over a

[#]This paper is based on work presented at the 6th Pacific Rim Conference on Rheology, held in the University of Melbourne, Australia from 20th to 25th July 2014.
*Corresponding author; E-mail: kyuhyun@pnu.ac.kr

specific blend ratio where the dispersed phase domain size is narrow enough to be calculated. It was shown that increasing the dispersed phase concentration (PBSA) induces co-continuity and gel-like behavior.

Processing conditions, blend ratios, viscosity ratios, and compatibilizers *etc.* are known to alter morphologies and rheological properties (Halimatudahliana *et al*., 2002; Salehiyan *et al*., 2014a; Salehiyan *et al*., 2014b). Stabilized morphologies and finer droplet dispersions can be obtained when coalescence is hindered and interfacial tension is reduced by addition of compatibilizers. Recently, inorganic fillers have attracted much interests due to their compatibilization effects (Wang *et al*., 2003; Ray *et al*., 2004; Hong *et al*., 2007; Cassagnau, 2008; Huitric *et al*., 2009; Cho *et al*., 2011; Zonder *et al*., 2011; Labaume *et al*., 2013; Salehiyan *et al*., 2015; Salehiyan and Hyun, 2013; Salehiyan *et al*., 2014a). Compatibilization effects of Cloisite30B (C30B, organoclay) on morphological and rheological properties of PE/PA-12 blends at different blend ratios were studied by Huitric *et al*. (2009). It was revealed that addition of C30B leads to corresponding reductions in domain size and interfacial tension for both PE- and PA-enriched blends regardless of the mechanism. Moreover, high concentration of PA-enriched blends show solid-like behavior due to high dispersity of C30B in favorable PA phase. Lately, the effects of two different particles Cloisite20A and AerosilOX50 (clay and silica), on non-linear rheological and morphological properties of (80/20) PP/PS blends were studied (Salehiyan *et al*., 2014a). It was found that clay particles located at the interface reduced droplet size and interfacial tensions. On the other hand, silica particles formed aggregates inside PS phase and did not improve morphological or rheological properties. Interestingly, non-linear rheological analysis of these blends captured differences in morphologies, whereas the linear rheological response increased the moduli due to volumetric effects of the fillers. Therefore, study properties within non-linear regions could provide information on material structures. Fourier transform (FT)-Rheology is known to be a promising tool to detect small changes in topology and morphology of materials (Hyun *et al*., 2007; Hyun and Wilhelm, 2009; Hyun and Kim, 2011, Hyun *et al*., 2011; Lim *et al*., 2013; Salehiyan and Hyun, 2013; Salehiyan *et al*., 2014a). FT-Rheology is a powerful method to quantify non-linear responses based on its sensitivity to stress signal.

Hence, in this study, morphological evolution of polypropylene/polystyrene (PP/PS) blends with different compositions was examined based on non-linear rheological properties under large amplitude oscillatory shear (LAOS) flow. The effects of Cloisite20A (C20A) as a compatibilizer on morphologies and rheological properties of corresponding blends were also investigated. FT-Rheology was used to quantify non-linear stress responses of polymer blends. FT-Rheology decomposes the stress data in time domains into the intensities in frequency domains (Wilhelm *et al*., 1998; 1999; 2000; Hyun *et al*., 2012). The third relative harmonic [$I_{3/1} \equiv I(3\omega)/I(\omega)$, where ω is the excitation frequency] was used as a non-linear parameter. Stress decomposition (SD) method was also applied for more precise characterization as it decomposes the total stress (σ) into elastic stress (σ') and viscous stress (σ''). Using SD method, elastic stress was more distorted, especially, strain hardening behavior, while the total stress response remained almost unchanged at larger strain amplitudes.

2. Experimental

2.1. Materials

Polypropylene (PP), (MI = 60.0 g/10 min at 230°C and load 2.16 kg, grade HP562T) with ($\overline{M_n}$ = 56,000, $\overline{M_w}$ = 157,100, PDI = 2.81), used in this study was obtained from PolyMirae Company Ltd. HP562T is a homopolymer particularly suitable for fine denier spunbonded nonwovens. Polystyrene (PS), (MI = 17.6 g/10 min at 230°C and load 3.8 kg, grade HF2680) with ($\overline{M_n}$ = 59,200, $\overline{M_w}$ = 168,700, PDI = 2.85), was provided from Samsung Cheil Industries Inc. The polymers are listed in Table 1. Organoclay, Cloisite20A (C20A), was purchased from Southern Clay Products Inc. Cloisite20A is a dimethyl-hydrogenated tallow ammonium-modified montmorillonite with a density of 1.77 g/cm^3 and particle sizes of (2-13 mm).

2.2. Blend preparations

Melt compounding of the blends was carried out in an internal Haake mixer (Rheocord 90) at 50 rpm and 180°C for 15 mins. The blend compositions were chosen as PP/

Table 1. Characteristics of the polymers.

Substance	Trademark	Characteristics	Supplier
PP (Polypropylene)	HP562T	MI = 60.0 g/10 min at 230°C and load 2.16 kg*	Polymirae
		Tensile strength at yield = 370 kg/cm^{2}**	
		Flexural modulus = 15,000 kg/cm^{2}***	
PS (Polystyrene)	HF2680	MI = 17.6 g/10 min at 230°C and load 3.8 kg****	Samsung Cheil Industries Inc.

*ASTM D1238L, **ASTM D638, ***ASTM D790, and ****ASTM D1238

PS (10/90, 30/70, 50/50, 70/30, and 90/10). Clay particles were added at 5 wt.% to the blends. After melt blending, pellets were compressed and molded into disks with a diameter of 25 mm and thickness of 1 mm at 180°C.

2.3. Rheological measurements

Strain controlled rheometer RMS800 (Rheometrics Inc.) with 25 mm parallel plate geometries were used to carry out rheological measurements. Small amplitude oscillatory shear (SAOS) tests were conducted to probe linear rheological properties at 180°C and at a fixed strain amplitude within linear regime. Non-linear rheological properties were obtained through strain sweep tests under large amplitude oscillatory shear (LAOS) flows with increasing strain amplitude from $\gamma_0 = 0.01$ to 10 at a fixed frequency of 1 rad/s.

2.4. Morphology

Field Emission Scanning Electron Microscopy (FE-SEM) observations were carried out using a JSM 6700F microscope at 5 kV to evaluate morphological evolutions. Samples were fractured in nitrogen liquid and then covered with platinum. The volume average radius (R_v) were calculated using Eq. (1). Radii were calculated using image analyzer software (ImageJ)

$$R_v = \frac{\Sigma n_i R_i^4}{\Sigma n_i R_i^3}, \quad (1)$$

where n_i is the number of droplets with radius R_i.

3. Result and Discussion

Small amplitude oscillatory shear (SAOS) tests were carried out at 180°C within the linear regime before large amplitude oscillatory shear (LAOS) tests. Storage moduli G'(ω) of the blends with and without clay (C20A) are shown in Fig. 1a and Fig. 1b. Elevation of the dispersed phase (PS) concentration increased the plateau modulus and width of this modulus. Form relaxation process applied to dispersed phase droplets (PS) during oscillatory shear deformations is known to cause non-terminal (plateau modulus) behavior at lower frequencies (Souza and Demarquette, 2002; Wu *et al*., 2008). The diameter of the dispersed phase changes as the concentration increases up to a composition within phase inversion (Co-continuous morphology), as does the interfacial area and relaxation process of corresponding blends. After this composition (50/50) PP/PS where matrix is changing from PP to PS, droplet size gradually decreases again. The storage modulus G' at ω = 10 rad/s of the PP/PS and PP/PS/5 wt.% C20A blends as a function of PP composition are depicted in Fig. 1c.

The solid line in Fig. 1c represents log additive mixing rule, $\log G' = \phi \log G'_{PP} + (1-\phi)\log G'_{PS}$ and the dash line

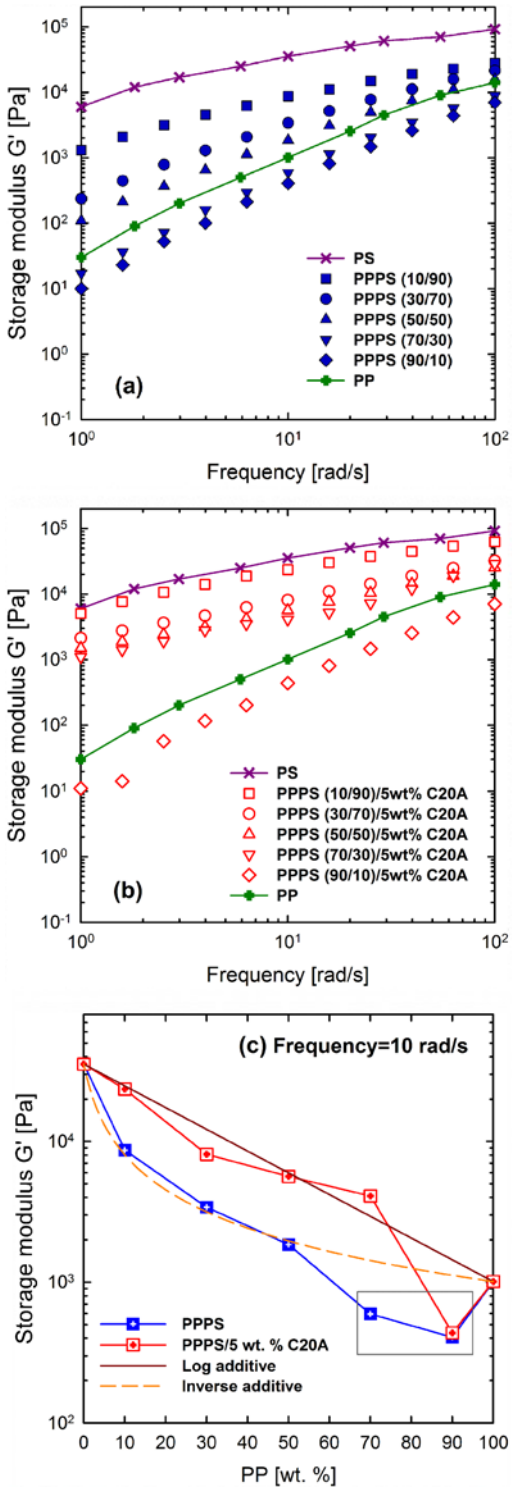

Fig. 1. (Color online) Storage moduli G'(ω) of the (a) PP/PS and (b) PP/PS/5 wt.% C20A blends as a function of frequency from 1 to 100 rad/s at strains within linear region and temperature of 180°C. (c) Comparison of the Storage moduli G'(ω) of the PP/PS blends with and without 5 wt.% C20A particles as a function of PP concentrations at a fixed frequency of 10 rad/s. The solid line represents log additive mixing rule and the dash line reciprocal (inverse) mixing rule.

reciprocal mixing rule $1/G' = \phi(1/G'_{PP}) + (1-\phi)(1/G'_{PS})$, respectively. The log additive mixing rule is a simple "general" mixing rule for polymer blends, reciprocal mixing rule is negative deviation (NDB) from the log additive mixing rule (Utracki, 1991). The reciprocal mixing rule represents the viscosity of an infinitely layered mixture of two Newtonian fluids (Grizutti *et al*., 2000). Thus PP/PS blend without clay can be better described by reciprocal mixing rule than PP/PS with clay, because clay can play as compatibilizer in immiscible PP/PS blend. The PP/PS/C20A can be described by log additive mixing rule. It is inferred that PP/PS/C20A blends have more dispersed phase than PP/PS blend as a consequence of suppressed coalescence (will be discussed). It is also interesting to note that storage moduli G'(ω) of the PP-enriched blends (90/10) and (70/30) PP/PS blends are lower than those of neat homopolymers (rectangular box in Fig. 1c). This phenomenon is believed to be due to interfacial slip effects (Utracki, 1991; Zhao and Macosko, 2002; Salehiyan *et al*., 2014b). Lower entanglement densities at interfacial areas in such cases bring about slippage, which leads to moduli values lower than those of virgin polymers. Further addition of 5 wt.% clay (C20A) significantly increased storage moduli of the blends and improved the interfacial slip effect in (70/30) PP/PS blend (Fig. 1c). However, in the case of (90/10) PP/PS blend, there was no change in the modulus, at least within the measured frequency range. Wu *et al*. (2000) reported that the storage modulus (G') of a filled polymer system is a combination of three effects: polymeric matrix itself, polymer-particle, and particle-particle effects. The latter is the main reason behind the non-terminal behavior of filled polymer systems at low frequencies. However, the current system is more complicated since dispersed phase droplets and clay (C20A) particles coexist in a polymer matrix. Therefore, a combination of droplet morphology (polymer-polymer interactions), clay (C20A) orientations (polymer-particle interactions), clay (C20A) (particle-particle interactions) and matrix itself will affect the rheological properties G'(ω) of the blends. It is known that clay (C20A) is more compatible with PS phase as previous study revealed increased inter-gallery spacing of PS/C20A nanocomposites due to clay intercalation (Cho *et al*., 2011). It is expected that the interfacial area undergoes changes following clay (C20A) incorporations, leading to different droplet sizes (Salehiyan *et al*., 2014a). Clay (C20A) particles can act as compatibilizers for PP/PS blends, leading to growth of moduli G'(ω) specifically at low frequencies.

In order to probe the viscoelastic behaviors of blends at large deformations, LAOS tests were carried out at strain amplitudes from 0.01 to 10 and at a fixed frequency of 1 rad/s. Figs. 2a-2c shows the complex moduli $G^*(\gamma_0)$ and normalized complex moduli $G^*(\gamma_0)$ of the blends with and without clay (C20A) particles under LAOS flow. Increasing the dispersed phase (PS) concentrations increased the complex moduli of the blends. Moreover, incorporation of 5 wt.% clay (C20A) particles significantly elevated the moduli of the blends compared to those of their un-filled counterparts. Fig. 2c reveals more interesting results from a different perspective. In the case of un-filled blends,

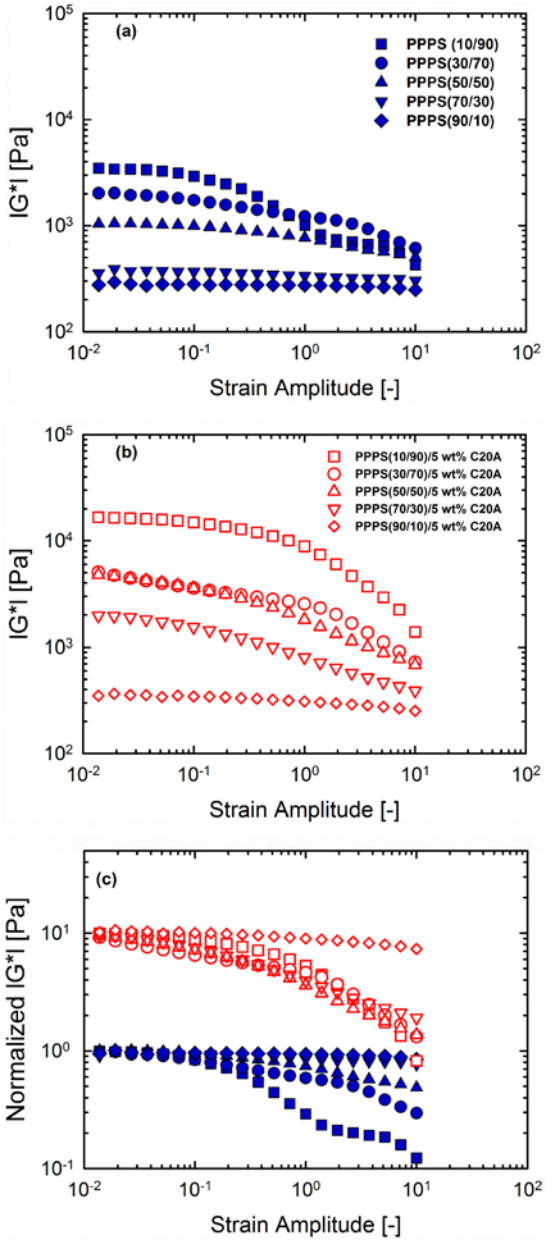

Fig. 2. (Color online) Complex moduli $G^*(\gamma_0)$ of the (a) PP/PS (b) PP/PS/5 wt.% C20A and (c) Normalized complex moduli $G^*(\gamma_0)$ of the blends with and without clay (C20A) particles under LASO flow at 180°C and fixed frequency of 1 rad/s. The normalized complex moduli of the blends with 5 wt.% C20A have been artificially shifted by a factor of 10 in Fig. 2c for the sake of clarity. Open and solid symbols are accounted for blends with and without clay (C20A) particles, respectively.

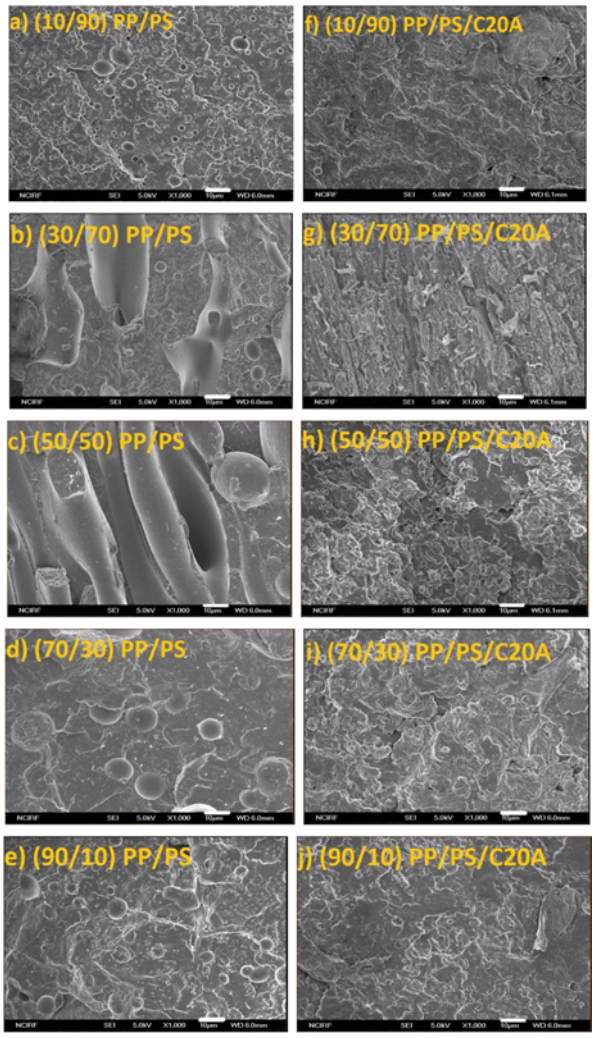

Fig. 3. (Color online) Morphological evolutions of the PP/PS blends (a) (10/90) PP/PS, (b) (30/70) PP/PS, (c) (50/50) PP/PS, (d) (70/30) PP/PS, (e) (90/10) PP/PS, (f) (10/90) PP/PS/5 wt.% C20A, (g) (30/70) PP/PS/5 wt.% C20A, (h) (50/50) PP/PS/5 wt.% C20A, (i) (70/30) PP/PS/5 wt.% C20A, and (j) (90/10) PP/PS/5 wt.% C20A. Scale bar is 10 μm for all the figures.

increasing the dispersed phase (PS) concentrations promoted the strain thinning behavior as (10/90) PP/PS blend showed the strongest strain thinning behavior. This is consistent with the work by Ziegler and Wolf (1999), who reported that less deformable droplets result in weaker shear thinning behavior. As shown in Fig. 1, PP is the more deformable phase, as its storage modulus G'(ω) is much lower than that of PS homopolymer. Therefore, PP droplets in (10/90) PP/PS blend would deform easier when sheared in PS matrix, resulting in stronger strain thinning behavior. On the other hand, weaker strain thinning behavior in the (90/10) PP/PS blend could be explained by less deformable phase (PS) undergoing shear in PP matrix. As a result, (10/90) PP/PS blend has lower

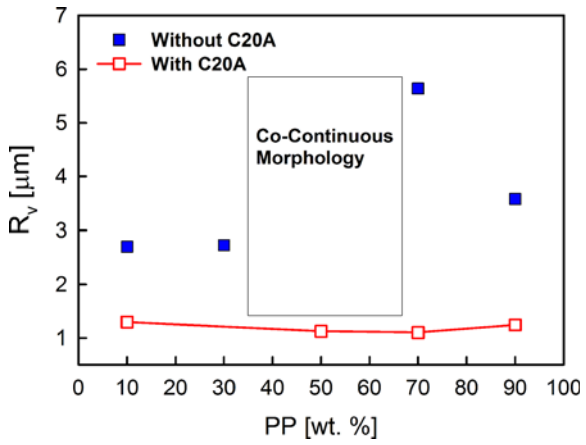

Fig. 4. (Color online) Volume average droplet radii R_v of the PP/PS and PP/PS/5 wt.% C20A blends as a function of PP content.

droplet sizes compared to (90/10) PP/PS blend (See Figs. 3 and 4). Interestingly, when clay (C20A) particles were added to blends, their corresponding nanocomposites showed the same shear thinning behavior, except for (90/10) PP/PS blends in which strain thinning remained unchanged. This is, clay (C20A) incorporation improved the rheological properties of PP/PS blends. Volume average droplet radii of the blends with and without clay (C20A) are plotted in Fig. 4.

Different mechanisms of droplet size reduction are expected for PP- and PS-enriched blends. Previous studies have revealed that clay (C20A) locates at the interface between PP and PS phases and prevents coalescence of the droplets by creating repulsive forces in PP-enriched (80/20) PP/PS blend (Salehiyan *et al*., 2014a). Excessive clay (C20A) particles at high concentrations are located inside PS phase due to more compatibility with PS. Therefore, dispersion of clay (C20A) particles in PS matrix for-

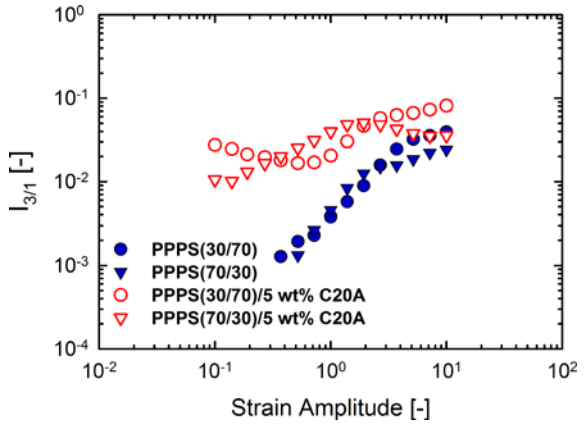

Fig. 5. (Color online) Normalized third relative ($I_{3/1}$) intensities of (30/70) and (70/30) PP/PS blends with and without 5 wt.% (C20A) particles.

tifies reduction of PP droplet sizes by altering the viscosity of the matrix. This leads to more solid-like behavior, similar to those of compatibilized blend systems.

Several methods have been introduced to analyze non-linear rheological responses (Hyun *et al*., 2011). In this study FT-Rheology was used to quantify the non-linear responses of the blends. Normalized third relative intensities ($I_{3/1}$) of the (30/70) and (70/30) PP/PS blends with and without 5 wt.% clay (C20A) are shown in Fig. 5. It is well known that $I_{3/1}$ is quite sensitive to internal structures of materials (Filipe *et al*., 2004; Hyun and Wilhelm, 2009; Wagner, 2011; Hyun *et al*., 2012; Hyun and Kim, 2012; Hyun *et al*., 2013; Lim *et al*., 2013; Salehiyan and Hyun, 2013; Salehiyan *et al*., 2014a; Lee *et al*., 2015). Lim *et al*. (2013) concluded that non-linearity ($I_{3/1}$) is related with interfacial properties of the polymer nanocomposite. Reinheimer *et al*. (2011) revealed that ($I_{3/1}$) is related with the inverse of interfacial tension according to their theoretical model for emulsion systems.

In this study, 5 wt.% clay (C20A) significantly increased the intensities of the blends. Previous studies revealed that increasing non-linearities ($I_{3/1}$) is an indication of a compatibilization effect in immiscible polymer blends (Salehiyan and Hyun, 2013; Salehiyan *et al*., 2014a). Moreover, these non-linearities increase when droplet sizes decrease in polymer blends. This supports SEM results that droplet size of the blends decreased upon clay (C20A) incorporation.

Lissajous curves are another method for studying non-linear stress under LAOS flow based on closed loops of normalized stress versus normalized strain (Ewoldt *et al*., 2008; Hyun *et al*., 2011). As these closed loops become more ellipsoidal, the response becomes more elastic. Lissajous curves of the blends and their nanocomposite counterparts are plotted in Figs. 6a and 6b at different strain amplitudes and blend ratios. Closed loops were more ellipsoidal at low strain amplitudes and lower PP concentrations, indicating a more elastic response when deformations were smaller and PS phase was dominant. Increasing strain amplitude and PP concentrations resulted in more viscous responses and the shape of loops became more circular where the viscous response is more dominant. Furthermore, when clay (C20A) particles were added, more elastic behavior was observed, and Lissajous curves became more ellipsoidal. This effect is more evident within the strain amplitudes and blend ratios, which are separated in a red box in Fig. 6b. Although it seems Lissajous curves can reflect the differences in viscoelasticity of polymer blends at different blend ratios and strain amplitudes, it is still difficult to distinguish the shape differences in some cases, especially at large strain amplitudes of different compositions.

Cho *et al*. (2005) proposed a method that decomposes the total stress response into elastic stress σ' and viscous

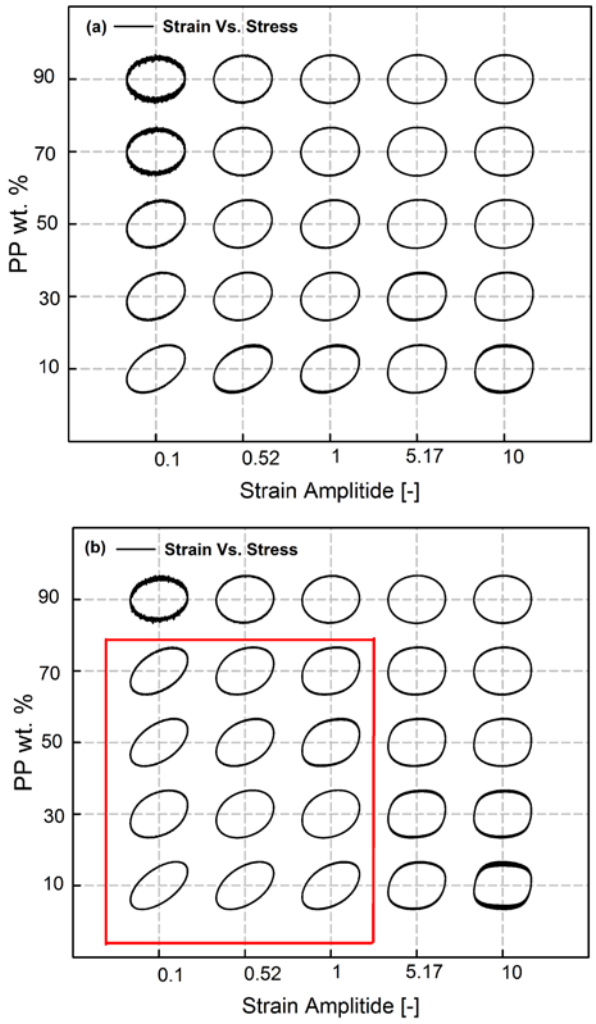

Fig. 6. (Color online) Normalized stress versus normalized strain (Lissajous plots) of (a) PP/PS and (b) PP/PS/5 wt.% C20A blends at a fixed frequency of 1 rad/s for different blend ratios at different strain amplitudes.

stress σ". By using this stress decomposition (SD) method, distortions at large deformations could be detected. For instance, SD method is applied to the (90/10) and (10/90) PP/PS (PP-enriched and PS-enriched) blends and (10/90) PP/PS/5 wt.% C20A blends to observe the effects of composition and clay (C20A) addition on non-linear stress response at large deformations (see Figs. 7a and 7b). Fig. 7a shows that distortion in normalized elastic stress (σ'/σ_{max}) was more evident while the normalized total stress (σ/σ_{max}) of the (10/90) and (90/10) PP/PS blends demonstrated nearly the same response. Due to elasticity of PS (see Fig. 1, G' of PS is larger than G' of PP), the elastic stress of (10/90) PP/PS show stronger strain hardening than (90/10) PP/PS. When 5 wt.% C20A is added to the (10/90) PP/PS blend, the normalized elastic stress (σ'/σ_{max}) show more noticeable strain hardening than (10/90) PP/PS blend without clay (see Fig. 7b). Clay play role as

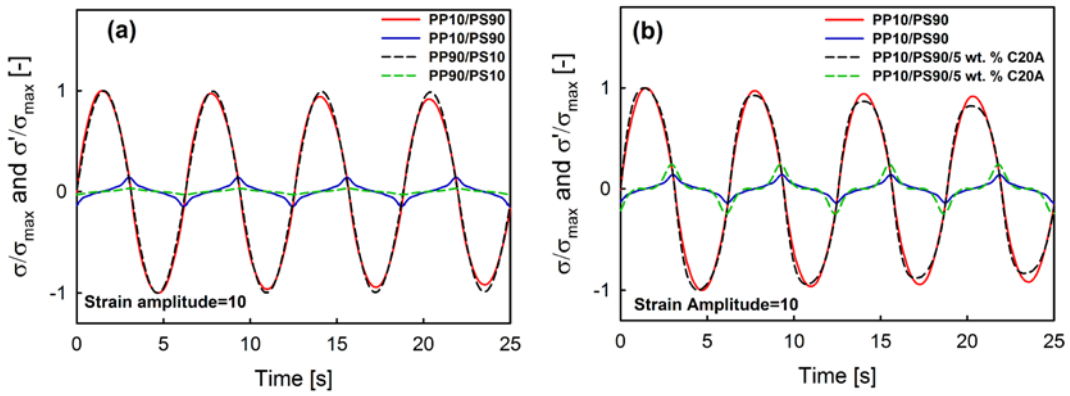

Fig. 7. (Color online) Normalized total stress σ/σ_{max} (red-solid line) and elastic stress σ'/σ_{max} (blue-solid line) of the (a) (10/90) and (90/10) PP/PS blends and (b) (10/90) PP/PS and (10/90) PP/PS/5 wt.% C20A blends at a strain amplitude of 10.

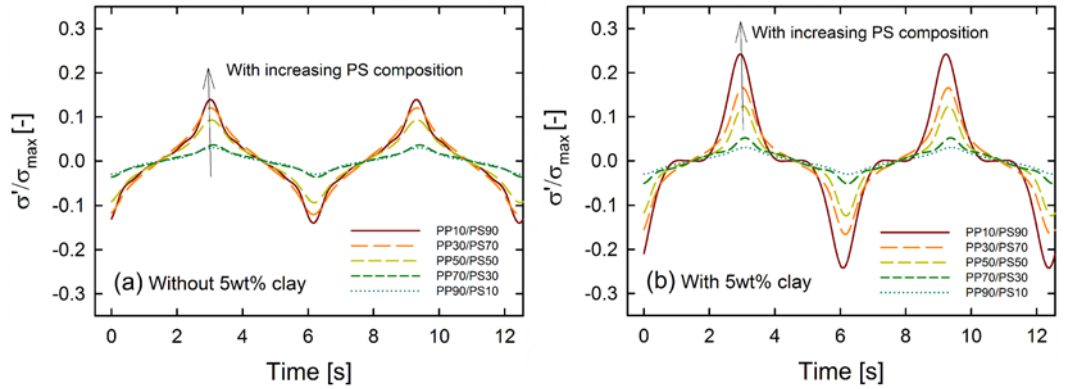

Fig. 8. (Color online) Normalized elastic stress σ'/σ_{max} of the (a) PP/PS blends without 5 wt.% C20A (b) PP/PS with 5 wt.% C20A at the strain amplitude of 10.

compatibilizers, the well dispersed phase can make strain hardening of elastic stress. For further studying elastic stress, the normalized elastic stresses are compared in Fig. 8 (PP/PS blends without clay in Fig. 8a and with clay in Fig. 8b). At large strain amplitude ($\gamma_0 = 10$), the elastic stress show strain hardening. With PS composition increase, elastic stress become large due to elasticity of PS. At same composition, the blends with clay show stronger strain hardening than without clay. The well dispersed phase by clay can make stronger strain hardening.

From above results, non-linear rheological analysis could be promising method to investigate microstructural evolutions of the blends. However, further investigation is required to probe the non-linearity of different blend ratios. Moreover, non-linear analyses based on total stress responses ($I_{3/1}$, Lissajous closed loops) could sometimes suffer from lack of precision, and that is where analysis based on stress decomposition could be useful.

4. Conclusion

Rheological and morphological properties of PP/PS and PP/PS/5 wt.% C20A blends at different composition ratios were studied. Small amplitude oscillatory shear (SAOS) test was used to study the linear viscoelastic behavior of the blends and non-linear rheological properties were examined through large amplitude oscillatory shear (LAOS) tests. In both SAOS and LAOS results, increasing dispersed phase (PS) concentrations increased viscoelasticity and strain thinning behavior of the blends. This was consistent with domain size reduction where low viscous droplets (PP) in high viscous matrix (PS) phase easily deformed under the shear flow, leading to the lowest droplet size and highest viscoelasticity in (10/90) PP/PS blends. Furthermore, addition of 5 wt.% clay (C20A) significantly improved the morphologies and rheological properties of the blends, regardless of the compatibilization mechanisms. This suggests that it could be coalescence inhibition due to encapsulation of PS droplets in PP matrix or size reduction due to changes in PS matrix viscosity, which favors the break-up of PP domains into smaller sizes. Interestingly, clay (C20A) additions lead to the similar shear thinning behavior for all blends except for (90/10) PP/PS/ 5 wt.% C20A blend in which rheological prop-

erties remained unchanged despite the morphological improvements. Furthermore, non-linear rheological analysis of (30/70) and (70/30) PP/PS blends with and without clay (C20A) via FT-rheology methods proved the compatibilization effect of clay (C20A) particles when inverse correlation between nonlinearity ($I_{3/1}$) and droplet size exists. Finally, stress decomposition method could be a powerful tool to more precisely examine the non-linear responses. Furthermore, it is necessary to investigate other properties also to examine effect of organo-modified clay, for example, impact strength, TGA analysis, resistance against degradation when clay added.

Acknowledgements

This research was supported by the Basic Science Research Program through the National Research Foundation of Korea (NRF) (No. 2010-0024466) and Global Ph. D. Fellowship Program through the National Research Foundation of Korea (NRF) funded by the Ministry of Education (2014H1A2A1015767).

References

Asthana, H. and K. Jayaraman, 1999, Rheology of Reactively Compatibilized Polymer Blends with Varying Extent of Interfacial Reaction, *Macromolecules* **32**, 3412-3419.

Cassagnau, P., 2008, Melt rheology of organoclay and fumed silica nanocomposites, *Polymer* **49**, 2183-2196.

Cho, K.S., K. Hyun, K.H. Ahn, and S.J. Lee, 2005, A geometrical interpretation of large amplitude oscillatory shear response, *J. Rheol.* **49**, 747-758.

Cho, S., J.S. Hong, S.J. Lee, K.H. Ahn, J.A. Covas, and J.M. Maia, 2011, Morphology and rheology of polypropylene/polystyrene/clay nanocomposites in batchand continuous melt mixing processes, *Macromol. Mater. Eng.* **296**, 341-348.

Elias, L., F. Fenouillot, J.C. Majeste, and P. Cassagnau, 2007, Morphology and rheology of immiscible polymer blends filled with silica nanoparticles, *Polymer* **48**, 6029-6040.

Elias, L., F. Fenouillot, J.C. Majeste, P. Alcouffe, and P. Cassagnau, 2008, Immiscible polymer blends stabilized with nanosilica particles: Rheology and effective interfacial tension, *Polymer* **49**, 4378-4385.

Ewoldt, R.H., A.E. Hosoi, and G.H. McKinley, 2008, New measures for characterizing nonlinear viscoelasticity in large amplitude oscillatory shear, *J. Rheol*. **52**, 1427-1458.

Filipe, S., M.T. Cidade, M. Wilhelm, and J.M. Maia, 2006, Evolution of the morphological properties along the extruder length for compatibilized blends of a commercial liquid crystalline polymer and polypropylene, *J. Appl. Polym. Sci.* **99**, 347-359.

Gleinser, W., H. Braun, Chr. Friedrich, and H.J. Cantow, 1994, Correlation between rheology and morphology of compatibilized immiscible blends, *Polymer* **35**, 128-135.

Grizutti, N., G. Buonocore, and G. Iorio, 2000, Viscous behavior and mixing rules for an immiscible model polymer blend, *J. Rheol.* **44**, 149-164.

Gui, Z.Y., H.R. Wang, Y. Gao, C. Lu, and S.J. Cheng, 2012, Morphology and melt rheology of biodegradable poly(lactic acid)/poly(butylene succinate adipate) blends: effects of blend compositions, *Iran. Polym. J.* **21**, 81-89.

Halimatudahliana, A., H. Ismail, and M. Nasir, 2002, Morphological studies of uncompatibilized and compatibilized polystyrene/polypropylene blend, *Polym. Test* **21**, 263-267.

Hong, J.S., Y.K. Kim, K.H. Ahn, S.J. Lee, and C. Kim, 2007, Interfacial tension reduction in PBT/PE/clay nanocomposite, *Rheol. Acta* **46**, 469-478.

Huitric, J., J. Ville, P. Mederic, M. Moan, and T. Aubry, 2009, Rheological, morphological and structural properties of PE/PA/nanoclay ternary blends: Effect of clay weight fraction, *J. Rheol.* **53**, 1101-1119.

Hyun, K., E.S. Baik, K.H. Ahn, S.J. Lee, M. Sugimoto, and K. Koyama, 2007, Fourier-transform rheology under medium amplitude oscillatory shear for linear and branched polymer melts, *J. Rheol*. **51**, 1319-1342.

Hyun, K., H.T. Lim, and K.H. Ahn, 2012, Nonlinear response of polypropylene (PP)/Clay nanocomposites under dynamic oscillatory shear flow, *Korea-Aust. Rheol. J.* **24**, 113-120.

Hyun, K. and M. Wilhelm, 2009, Establishing a new mechanical nonlinear coefficient Q from FT-rheology: first investigation on entangled linear and comb polymer model systems, *Macromolecules* **42**, 411-422.

Hyun, K., M. Wilhelm, C.O. Klein, K.S. Cho, J.G. Nam, K.H. Ahn, S.J. Lee, R.H. Ewoldt, and G.H. McKinley, 2011, A review of nonlinear oscillatory shear tests: analysis and application of large amplitude oscillatory shear (LAOS), *Prog. Polym. Sci.* **36**, 1697-1753.

Hyun, K. and W. Kim, 2011, A new non-linear parameter Q from FT-Rheology under nonlinear dynamic oscillatory shear for polymer melts system, *Korea-Aust. Rheol. J.* **23**, 227-235.

Hyun, K., W. Kim, S.J. Park, and M. Wilhelm, 2013, Numerical simulation results of the nonlinear coefficient Q from FT-Rheology using a single mode pom-pom model, *J. Rheol.* **57**, 1-24.

Labaume, I., P. Mederic, J. Huitric, and T. Aubry, 2013, Comparative study of interphase viscoelastic properties in polyethylene/polyamide blends compatibilized with clay nanoparticles or with a graft copolymer, *J. Rheol.* **57**, 377-392.

Lee, S.H., H.Y. Song, K. Hyun, and J.H. Lee, 2015, Nonlinearity from FT-rheology for liquid crystal 8CB under large amplitude oscillatory shear (LAOS) flow, *J. Rheol.* **59**, 1-19.

Lim, H.T., K.H. Ahn, S.J. Lee, J.S. Hong, and K. Hyun, 2013, Nonlinear viscoelasticity of polymer nanocomposites under large amplitude oscillatory shear flow, *J. Rheol.* **57**, 767-789.

Macaubas, P.H.P., N.R. Demarquette, and J.M. Dealy, 2005, Nonlinear viscoelasticity of PP/PS/SEBS blends, *Rheol. Acta* **44**, 295-312.

Ray, S.S., S. Pouliot, M. Bousmina, and L.A. Utracki, 2004, Role of organically modifed layered silicate as an active interfacial modifer in immiscible polystyrene/polypropylene blends, *Polymer* **45**, 8403-8413.

Reinheimer, K., M. Grosso, and M. Wilhelm, 2011, Fourier Transform Rheology as a universal non-linear mechanical characterization of droplet size and interfacial tension of dilute

monodisperse emulsions, *J. Colloid Interface Sci.* **360**, 818-825.

Salehiyan, R., A.A. Yussuf, N.F. Hanani, A. Hassan, and A. Akbari, 2015, Polylactic acid/polycaprolactone nanocomposite: influence of montmorillonite and impact modifier on mechanical, thermal and morphological properties, *J. Elastomers. Plast.* **47**, 69-87.

Salehiyan, R. and K. Hyun, 2013, Effect of organoclay on nonlinear rheological properties of poly(lactic acid)/poly(caprolactone) blends, *Korean J. Chem. Eng.* **30**, 1013-1022.

Salehiyan, R., Y. Yoo, W.J. Choi, and K. Hyun, 2014a, Characterization of morphologies of compatibilized polypropylene/polystyrene blends with nanoparticles via nonlinear rheological properties from FT-rheology, *Macromolecules* **47**, 4066-4076.

Salehiyan, R., W.J. Choi, J.H. Lee, and K. Hyun, 2014b, Effects of mixing protocol and mixing time on viscoelasticity of compatibilized PP/PS blends, *Korea-Aust. Rheol. J.* **26**, 311-318.

Souza, A.M.C. and N. R. Demarquette, 2002, Influence of composition on the linear viscoelastic behavior and morphology of PP/HDPE blends, *Polymer* **43**, 1313-1321.

Utracki, L.A., 1991, On the viscosityconcentration dependence of immiscible polymer blends, *J. Rheol.* **35**, 1615-1637.

Van Puyvelde, P., S. Velankar, and P. Moldenaers, 2001, Rheology and morphology of compatibilized polymer blends, *Curr. Opin. Colloid Interface Sci.* **6**, 457-463.

Wagner, M.H., V.H. Rolón-Garrido, K. Hyun, and M. Wilhelm, 2011, Analysis of medium amplitude oscillatory shear (MAOS) data of entangled linear and model comb polymers, *J. Rheol.* **55**, 495-516.

Wang, Y., Q. Zhang, and Q. Fu, 2003, Compatibilization of immiscible poly(propylene)/polystyrene blends using clay, *Macromol. Rapid Commun.* **24**, 231-235.

Wilhelm, W., D. Maring, and H.W. Spiess, 1998, Fourier-transform rheology, *Rheol. Acta* **37**, 399-405.

Wilhelm, W., P. Reinheimer, and M. Ortseifer, 1999, High sensitivity Fourier-transform rheology, *Rheol. Acta* **38**, 349-356.

Wilhelm, W., P. Reinheimer, M. Ortseifer, T. Neidhofer, and H.W. Spiess, 2000, The crossover between linear and non-linear mechanical behaviour in polymer solutions as detected by Fourier-transform rheology, *Rheol. Acta* **39**, 241-246.

Wu, G., S. Asai, M. Sumita, T. Hattori, R. Higuchi, and J. Washiyama, 2000, Estimation of flocculation structure in filled polymer composites by dynamic rheological measurements, *Colloid. Polym. Sci.* **278**, 220-228.

Zhao, R. and C.W. Macosko, 2002, Slip at polymer-polymer interfaces: Rheological measurements on coextruded multilayers, *J. Rheol.* **46**, 145-167.

Ziegler, V. and B.A. Wolf, 1999, Viscosity and morphology of the two-phase system PDMS/P(DMS-ran-MPS), *J. Rheol.* **43**, 1033-1045.

Zonder, L., A. Ophir, S. Kenig, and S. McCarthy, 2011, The effect of carbon nanotubes on the rheology and electrical resistivity of polyamide 12/high density polyethylene blends, *Polymer* **52**, 5085-5091.